Comparison of Cylindrical and Spherical Mathematical Absorber Reflection Suppression

S.F. Gregson[1], A.C. Newell[2], G.E. Hindman[3], M.J. Carey[4]

Nearfield Systems Inc.
19730 Magellan Drive, Torrance, CA 90502, USA

[1]sgregson@nearfield.com
[2]anewell@nearfield.com
[3]ghindman@nearfield.com
[4]mcarey@nearfield.com

***Abstract*— Reflections in antenna test ranges can often constitute the largest single term within the error budget of a given facility [1]. For some time, a frequency domain measurement and post-processing technique named Mathematical Absorber Reflection Suppression (MARS) has been successfully used to reduce range multi-path effects within spherical near-field and far-field antenna measurement systems [2, 3, 4]. More recently, a related technique has been developed for use with cylindrical near-field antenna measurement systems [5, 6, 7]. This paper provides an introduction to the measurement techniques and a description of the novel near-field to far-field transform algorithms before presenting preliminary results of actual range measurements of a low gain antenna taken using a combination spherical / cylindrical system that was installed within a partially anechoic chamber. These results illustrate the success of the techniques which are found to provide comparable improvements yielding far-field patterns that are in encouraging agreement despite every step within the data acquisition, transformation and post-processing chain being different thereby providing further compelling evidence of the success of the MARS technique.**

I. INTRODUCTION

The spherical Mathematical Absorber Reflection Suppression (S-MARS) technique was first implemented to support operations in a large hemi-spherical automotive near-field test system that NSI installed for Nippon Antenna (now Antenna Technology Center Europe) in Itzehoe Germany [2, 8]. Without the S-MARS capability, scattering from the metallic floor and dielectric gantry and radome could otherwise have degraded the quality of the results obtained from the test system. Following on from this, the S-MARS technique was extended so that it could be used with other, more conventional spherical near-field antenna test systems. Here, it was found that the technique was sufficiently general to be used with: polar and equatorial mode acquisitions, robotics positioning sub-systems utilising "model tower" ϕ/θ and "scanning arm" θ/ϕ arrangements, and to characterise linear and circularly polarised antennas, enabling meaningful results to be obtained from systems containing limited or even no absorber at all, as well as for use in improving the reflection performance in a traditional anechoic chamber. The sheer number and variety of measurement configurations and antennas that were found to be helped by the MARS technique indicated that the physical principle that underpinned the process might be sufficiently general in form to be extended to other measurement geometries. Thus, as the cylindrical near-field methodology was thought to be conceptually most closely related to the spherical case, and although the mathematical treatment is entirely distinct, cylindrical MARS (C-MARS) was implemented essentially as a corollary to S-MARS [5, 6, 7]. In this way, it was found that the underlying MARS technique was not a peculiarity of one or other modal basis or sampling scheme, *etc.*. Thus, although the actual mathematical operators *are* peculiar to the particular experimental geometry concerned, the underlying physical principles that enables a distinction to be made between those fields that are associated with the AUT and those arising from scattering, are not. In each of the spherical and cylindrical implementations: a unique measurement and mathematical post processing technique is implement that requires only a minimum amount of detailed information about the AUT probe and range geometry, the processing is applied during the near-field to far-field transformation and a mathematical operator is applied to the measured data that orthogonalises those field associated with the AUT from those fields associated with other spurious sources so that unwanted contributions can be effectively filtered out. But every step in the measurement and data processing chains for the two geometries are independent and different. This paper highlights this fact by comparing and contrasting the respective measurement and data processing chains before presenting comparison measurements taken of a low gain AUT in a combination NSI-300V-12x12-PCS near-field antenna test system.

II. OVERVIEW OF THE MARS TECHNIQUE

It is well known that the electromagnetic fields outside an arbitrary test antenna radiating into free space can be expanded onto a set of elementary orthogonal spherical or cylindrical mode coefficients and that these modes and coefficients can then be used to obtain the electric and magnetic fields everywhere in space outside of respectively, a conceptual spherical or right circular cylindrical surface which encloses that radiator using modal orthogonality and the principle of linear superposition [9, 10]. These measurement geometries are presented below in Figures 1 and 2.

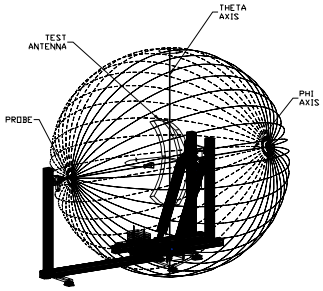

Fig. 1 Spherical positioning system and measurement geometry

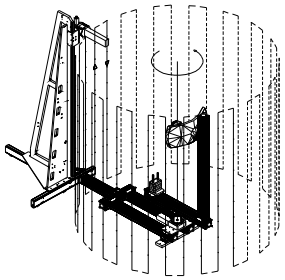

Fig. 2 Cylindrical positioning system and measurement geometry

Each of these measurement configurations allow near-field data to be acquired on a raster scan over the conceptual measurement surfaces by holding the measurement radius constant with the θ- and ϕ-axes (or ϕ- and z-axes) being varied whilst the probe polarisation (χ-axis) is sequentially set to 0° and 90° to sample two tangential orthogonal near electric field components. The measured $\chi = 0°$, *i.e.* horizontally polarised, electric field components can be seen presented as three-dimensional virtual reality false colour plots in Figures 3 and 4 below.

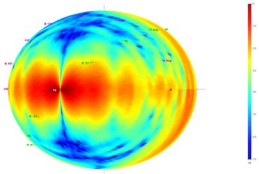

Fig. 3 Horizontally polarised measured spherical near-field component

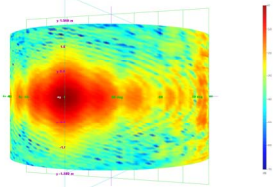

Fig. 4 Horizontally polarised measured cylindrical near-field component

These fields, together with their attendant orthogonal counterparts are used to obtain the spherical and cylindrical mode expansions respectively [9, 10]. The transverse electric (TE) spherical and cylindrical mode coefficients power spectra can be seen presented below in Figures 5 and 6 respectively. For a fixed measurement radius and frequency, these mode coefficients are complex numbers that do not vary with any of the scanning co-ordinates and are instead functions of the polarization index s. For the case of spherical mode coefficients (SMCs) they are also functions of the polar index n and the azimuthal index m such that $0 \le n \le \infty$ and $-n \le m \le n$ (which is why Figure 5 contains undefined regions denoted by white space). Conversely, for the case of cylindrical mode coefficients (CMCs) they are functions of n the angular index, and γ the Fourier variable which is the conjugate of the linear spatial variable z, such that $-\infty \le n \le \infty$, $-\infty \le \gamma \le \infty$.

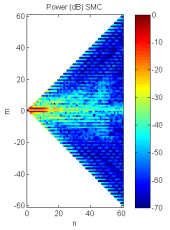

Fig. 5 Power pattern of TE SMCs

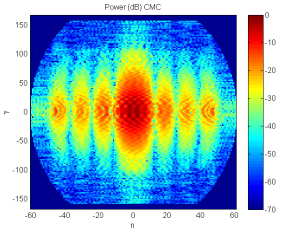

Fig. 6 Power pattern of TE CMCs

Here, due to the exponential decrease in the reactive modes only mode coefficients corresponding to polar indices less than the product of the free-space propagation constant and the maximum radial extent (k_0a) are computed. Similarly, the Fourier variable is limited to $\pm k_0$. For each of these cases, the spatial filtering characteristic of the near-field probe is compensated for by adjusting the complex amplitudes of the mode coefficients where it is recognised that a priori to a near-field measurement, the probe radiation properties must be known. Thus, as far-field, near-field, gain and polarization ratios can be found from the spherical or cylindrical mode coefficients, determining these mode coefficients for a given antenna is the goal of the near-field measurement process.

Classically, when making an antenna measurement, the AUT is installed within the near-, or far-field facility such that it is displaced in space as little as possible during the course of a measurement. As range multi-path tends to disturb the fields illuminating the test antenna, the purpose of this strategy is to insure that the field illuminating the test antenna changes as little as possible during the course of the acquisition. However, the MARS measurement technique adopts a fundamentally opposing strategy where by the test antenna is deliberately displaced from the centre of rotation. This has the effect of making the differences in the illuminating field far more pronounced than would otherwise be the case allowing more effective identification and removal of spurious fields. Thus, the data transformation and processing for a MARS measurement requires that the standard technique be modified. Although a detailed mathematical treatment is left to the open literature [2, 3, 4, 5, 6, 7, 9, 10, 11] an overview of the generic MARS processing algorithm is described below:

1. Take the two orthogonal tangential electric near-field components and compute the mode coefficients for each polarisation index, s.
2. Solve for the AUT's unknown mode coefficients using previously computed probe pattern mode coefficients. These mode coefficients are generally obtained from an a priori probe pattern characterisation and a modal translation integral that places the probe at the measurement radius.
3. Compute the complete far electric field components from mode coefficients.
4. Apply a differential phase change to mathematically translate the AUT back to the origin of the measurement co-ordinate system.
5. Obtain the translated mode coefficients of the AUT for an AUT conceptually located at the origin of the measurement co-ordinate system.
6. Apply two-dimensional mode filtering function to suppress unwanted mode coefficients where the properties of the filter function are determined from the physical size of the AUT and the free space propagation number. These filtered spherical and cylindrical mode coefficient can be seen presented in Figure 7 and 8 below, *c.f.* Figure 5 and 6 above.
7. Compute the complete far electric field pattern from the filtered mode coefficients to obtain the MARS filtered AUT pattern

function. Calculate magnetic fields from the electric fields and the plane wave condition.

Hence, the MARS methodology is very closely related to that of the classical near-field measurement and transformation techniques using as it does the standard steps (*i.e.* step 1, 2, 3) and merely deploying them in a subtly different way (*i.e.* step 4 is conventionally used within microwave holographic metrology, step 5 closely related to step 1 and step 7 is the same as step 3). This is true for both spherical and cylindrical implementations. Thus, whilst it is clear that the details of the modal basis, probe compensation, and transformation algorithms will be different for each of the geometries, for any given radiator, the resulting electromagnetic six-vector outside the respective excluded regions of space must equate *exactly*.

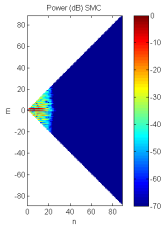

Fig. 7 AUT translated filtered power pattern of TE SMCs

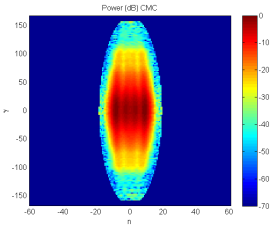

Fig. 8 AUT translated filtered power pattern of TE CMCs

However, errors such as range multi-path *etc.* [1], will impact upon the respective measurement systems in very different ways. The position and orientation of the AUT and near-field probe with respect to the chamber will be very different for the spherical and cylindrical cases and as such one would expect the effect that this has on the resulting error contaminated far-field pattern would also be very different. Thus, acquiring an antenna in a multi-path rich environment using both a spherical and a cylindrical measurement system where the uncorrected far-field patterns will inherently be very different would constitute a demanding test for the MARS technique.

III. Overview Of The Comparison Measurement

In order that the spherical and cylindrical MARS implementations could be effectively verified, an NSI-300V-12x12 combination planar/cylindrical/spherical (PCS) antenna measurement system was used to acquire a medium gain x-band standard gain horn (SGH). This system can be seen presented in Figure 9 below where the testing was conducted in a chamber where only the region behind the planar scan plane was lined with 36" (0.9 m) pyramidal absorber leaving the remaining floor, ceiling and walls exposed. Thus, when taking spherical and cylindrical near-field measurements, room scattering effects could become more significant for larger azimuth angles. Measurements were taken in spherical and cylindrical acquisition modes. In accordance with MARS requirements, to effectively identify and remove spurious scattering, the AUT was offset from the centre of rotation by 12", which was a little more than the largest dimension of the radiator [6, 11]. Although the displacement can be larger than this, for this measurement configuration a larger offset provides only very limited benefits, and lengthens acquisition times and increases the importance of precise and accurate range alignment. The conceptual minimum MRE for the AUT translated to the origin was 5" thus limiting the maximum polar mode index to $|n| < 21$ for the translated AUT.

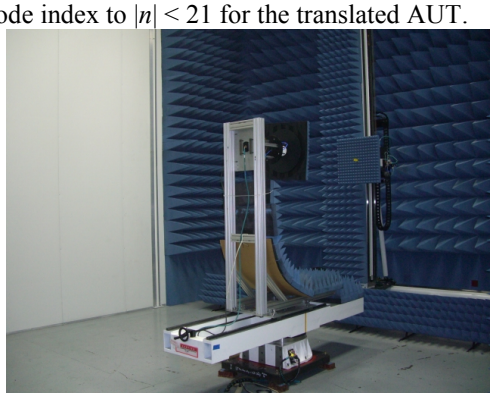

Fig. 9 NSI-300V-12x12 PCS system shown taking near-field measurements of NSI-RF-SG90 in a partially anechoic environment. Here, absorber placement has been optimised for planar acquisition mode.

Initially the near-field data was transformed to the far-field using conventional near-field processing. False colour plots of the far-field principle (Ludwig II azimuth) polarised field component can be found presented in Figures 11 and 12 for the spherical and cylindrical measurements respectively. These are shown as three-dimensional "virtual reality" polar plots. Figures 13 and 14 contain equivalent MARS filtered far-field antenna patterns. Here, the wide azimuth angle lobes can be seen to have been attenuated in both spherical and cylindrically derived far-field patterns. The high angular frequency ripple that was evident on the unprocessed patterns has also been suppressed. The wide elevation angle lobes that were evident on the spherical measurement have also been suppressed perhaps indicating that these too are artefacts of range reflections. An equivalent result would not be expected for the case of the cylindrical measurement as the onset of the first-order truncation effect would limit fields at large elevation angles.

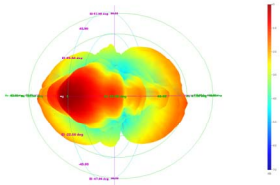

Fig. 10 Far-field pattern obtained from spherical measurement

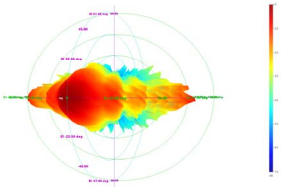

Fig. 11 Far-field pattern obtained from cylindrical measurement

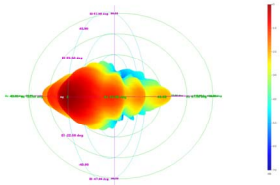

Fig. 12 Far-field pattern obtained from spherical measurement with spherical MARS processing

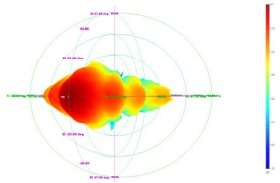

Fig. 13 Far-field pattern obtained from cylindrical measurement with cylindrical MARS processing

Thus, from inspection the spherical and cylindrical far-field patterns are in better agreement after MARS processing has been applied than they were before indicating the success of the technique. This qualitative observation is further

confirmed by quantitatively comparing the similarity of the far-field cardinal cuts obtained from the spherical and cylindrical measurement, both before and after MARS processing. Here, Figures 15 contains far-field azimuth cardinal cuts of the SGH obtained from spherical and cylindrical measurements. The purple trace is the difference between the two pattern measurements. Figure 16 contains a similar plot after spherical and cylindrical MARS processing had been applied. Figures 17 and 18 are equivalent plots for pattern measurements taken at the 12.4 GHz top of the waveguide 90 frequency band.

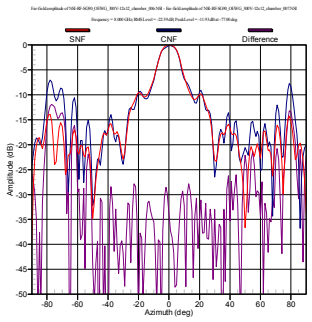

Fig. 14 Azimuth cuts from Spherical and cylindrical at 8.0 GHz without MARS processing

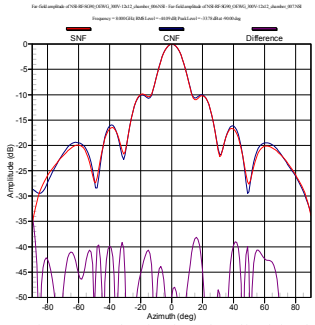

Fig. 15 Spherical and cylindrical azimuth cuts at 8.0 GHz with MARS processing

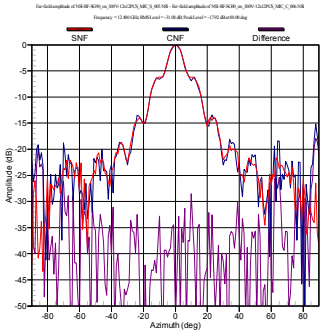

Fig. 16 Spherical and cylindrical azimuth cuts at 12.4 GHz without MARS processing

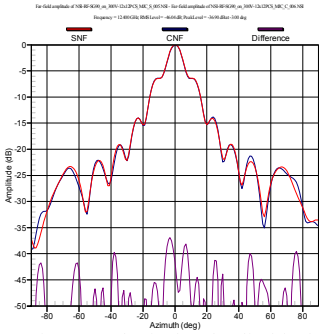

Fig. 17 Spherical and cylindrical azimuth cuts at 12.4 GHz with MARS processing

From inspection of Figure 14 and 15 it is clear that the difference level has improved significantly after MARS processing with the level decreasing by more than 10 dB on boresight, and by larger amounts at wider pattern angles with the wide out sidelobe structure that was hitherto obscured by multi-path subsequently becoming clearly revealed. A similar result is also evident at the top of the WR90 waveguide band, as shown in Figures 16 and 17 with the equivalent multi-path level (EMPL) being below -40 dB. It is important when reviewing these results to recognise that almost everything is different between cylindrical and spherical measurements and transformations and that the differences shown above contain not only difference from multi-path but additionally the respective uncertainties associated with each of the individual measurement systems.

IV. Summary And Conclusions

Spherical and cylindrical MARS processing can be used with a very high degree of confidence since all the steps in the measurement and analysis are consistent with the well established principles of the standard spherical and cylindrical near-field theory and measurement technique, and all comparisons to date have proved overwhelmingly positive. The offset of the AUT and the resulting smaller data point spacing are valid if the spacing satisfies the sampling criteria. The translation of the far-field pattern to the origin with the application of a differential phase shift is rigorous. The selection of the mode cut-off for the translated pattern is based on the physical dimensions of the AUT and its translated location. The results of the spherical and cylindrical MARS processing will reduce, but not entirely eliminate, the effect of the scattering. The final result with MARS processing can be degraded if the sampling of the near-field data is too coarse, or the mode filter is too tight, *i.e.* abrupt, but this is also true for regular spherical and cylindrical processing. Importantly, both of these parameters are controlled by the user and must be correctly specified. These frequency domain measurement and processing techniques are quite general and can be used to achieve acceptable results with use of minimal absorber or even without the use of an anechoic chamber. It can also improve the reflection levels in a traditional anechoic chamber allowing improved accuracy as well as offering the ability to use existing chambers down to lower frequencies than the absorber might otherwise indicate. Crucially, and for the first time, this paper has demonstrated the successful application of the MARS principle in spherical and cylindrical geometries thereby providing further compelling evidence of the validity of the underlying technique as all stages in the measurement, data transformation and post-processing chains are different, *e.g.* CME v SME, CMC filtering v SMC filtering, etc.). It should be noted however that this paper recounts the progress of an ongoing research study. Consequently, several issues remain to be addressed including obtaining similarly encouraging agreement between spherical, cylindrical and the new planar MARS technique (which is also under development).

References

[1] A.C. Newell, "Error Analysis Techniques for Planar Near-field Measurements", IEEE Transactions on Antennas and Propagation, vol. AP-36, pp. 754-768, June 1988.

[2] G.E. Hindman, A.C. Newell, "Reflection Suppression in a large spherical near-field range", AMTA 27th Annual Meeting & Symposium, Newport, RI, October. 2005.

[3] G.E. Hindman, A.C. Newell, "Reflection Suppression To Improve Anechoic Chamber Performance", AMTA Europe 2006, Munch, Germany, March 2006.

[4] G.E. Hindman, A.C. Newell, "Mission To MARS – In Search of Antenna Pattern Craters", AMTA 28th Annual Meeting & Symposium, St. Louis, MO, November 2007.

[5] S.F. Gregson, A.C. Newell, G.E. Hindman, "Reflection Suppression In Cylindrical Near-Field Antenna Measurement Systems – Cylindrical MARS", AMTA 31st Annual Meeting & Symposium, Salt Lake City, UT, November 2009.

[6] S.F. Gregson, A.C. Newell, G.E. Hindman, "Reflection Suppression In Cylindrical Near-Field Measurements of Electrically Small Antennas", Loughborough Antennas & Propagation Conference, November, 2009.

[7] S.F. Gregson, A.C Newell, G.E Hindman, M.J. Carey, "Advances in Cylindrical Mathematical Absorber Reflection Suppression", European Conference on Antennas and Propagation, Barcelona, April 2010.

[8] P. Betjes, D. Pototzki, D. van Rensubrg, "A hemispherical near-field system for automotive antenna testing", AMTA 27th Annual Meeting & Symposium, Newport, RI, Oct. 2005.

[9] J.E. Hansen (ed.), "Spherical Near-Field Antenna Measurements", IET, UK, Peter Peregrinus Ltd., 1988.

[10] A.D. Yaghjian, "Near-Field Antenna Measurements On a Cylindrical Surface: A Source Scattering Matrix Formulation", NBS Technical Note 696, 1977.

[11] G.E. Hindman, A.C. Newell, "Improving and Extending the MARS Technique to Reduce Scattering Errors", AMTA 31st Annual Meeting & Symposium, Salt Lake City, UT, November 2009.